Journal of Autoimmunity 151 (2025) 103372

Contents lists available at ScienceDirect

Journal of Autoimmunity

journal homepage: www.elsevier.com/locate/jautimm

Identification of clonally expanded T-cell receptor sequences in giant cell arteritis

Anna Weber [a,b,2], Michal Zulcinski [c,d,2], Lubna Haroon-Rashid [c,2], Beth Kuszlewicz [c], Alice Driessen [a,b], Darren Newton [c,d,1], Ann W. Morgan [c,d,*,1], María Rodríguez Martínez [a,e,1]

[a] International Buisness Machines Research Europe, Rüschlikon, 8803, Switzerland
[b] Eidgenössische Technische Hochschule Zurich, Department of Biosystems Science and Engineering (D-BSSE), 4058, Basel, Switzerland
[c] School of Medicine, University of Leeds, Leeds, LS2 9JT, UK
[d] NIHR Leeds Biomedical Research Centre, Leeds Teaching Hospitals NHS Trust, Leeds, UK
[e] Department of Biomedical Informatics & Data Science, Yale School of Medicine, New Haven, CT, United States

ARTICLE INFO

Handling editor: C Selmi

Keywords:
Giant cell arteritis
Vasculitis
T-cell receptor
T-cells
Pathogenesis

ABSTRACT

Background: Arterial wall inflammation in giant cell arteritis (GCA) is characterized by T-cell infiltration and granuloma formation. There have been limited studies investigating the diversity of the T-cell receptor (TCR) repertoire in GCA patients. Here we aim to identify disease-relevant TCRs.
Methods: We sequenced the TCRβ repertoires in peripheral blood and biopsies from 72 GCA patients and compared them to repertoires of 60 age-matched controls. Applying K-nearest neighbours classification based on tcrdist3, an established TCR similarity measure, we identified GCA-associated TCRs across multiple model hyperparameters and experimental replicates.
Results: We observed that species richness and Shannon diversity were significantly lower ($P = 0.0003$ and $P = 0.004$, respectively) in GCA peripheral blood TCR repertoires compared with age-matched controls. 1526 TCRs were identified that were consistently associated with GCA, 63 TCRs were also detected in TAB repertoires. Identical GCA-associated TCRs were observed in paired blood and tissue samples from 21/30 GCA cases. 57 % of GCA-associated TCRs were fitted into 10 clusters, which displayed distinct TCR sequences and TCR V and J segment usage. TRBV20-1*01, TRBV4-3*01, TRBV4-2*01 and TRBV4-1*01 segments were over-represented and occurred at least 10 % more often among GCA patients than age-matched controls. Only 27/1526 TCR sequences had matches reported in public databases, reducing the likelihood that these targeted common infectious agents.
Conclusions: Our data provide evidence of circulating T-cell clonal expansions in GCA patients. Certain TCR sequence patterns were over-represented in GCA subjects. As more TCR sequences directed at human antigens become available, further analysis may ultimately reveal whether these TCRs bind a common target antigen.

1. Introduction

Giant cell arteritis (GCA) is the commonest primary systemic vasculitis. GCA occurs exclusively in people over 50, and the incidence rises progressively with age [1]. Irreversible ischaemic complications have been reported in up to 17 % of patients in historical cohorts [2].

Abbreviations: CDR3, Complementary-determining region 3; GCA, Giant cell arteritis; FFPE, Formalin-fixed paraffin embedded; IMGT, International immunogenetics information system; K-NN, K-nearest neighbour; MAF, Minor allele frequency; MHC, Major histocompatibility complex; nDCG, Normalized discounted cumulative gain; PMR, Polymyalgia rheumatica; PNH, Paroxysmal nocturnal haemoglobinuria; TAB, Temporal artery biopsy; TCR, T-cell receptor; UMAP, Uniform manifold approximation and projection.

* Corresponding author. Leeds Institute of Cardiovascular and Metabolic Medicine, LIGHT Building, University of Leeds, Leeds, LS2 9JT, UK.
E-mail addresses: a92.weber@t-online.de (A. Weber), m.zulcinski@leeds.ac.uk (M. Zulcinski), L.HaroonRashid@leeds.ac.uk (L. Haroon-Rashid), bethanykuszlewicz@btinternet.com (B. Kuszlewicz), adr@zurich.ibm.com (A. Driessen), d.j.newton@leeds.ac.uk (D. Newton), a.w.morgan@leeds.ac.uk (A.W. Morgan), maria.rodriguezmartinez@yale.edu (M. Rodríguez Martínez).
[1] Equal contributions and to be considered joint Senior Authors.
[2] Equal contributions and to be considered joint first authors.

https://doi.org/10.1016/j.jaut.2025.103372
Received 29 August 2024; Received in revised form 16 January 2025; Accepted 21 January 2025
Available online 3 February 2025

GCA was traditionally considered a self-limiting cranial vasculitis. However, many patients have frequent relapses, develop progressive arterial stenoses, or late aortic dilatation. Patients have a 17-fold increased risk of thoracic aortic aneurysm, dissection and rupture [3]. A prolonged course of high-dose glucocorticoids remained standard therapy until 2022 when tocilizumab, an IL-6 receptor inhibitor, was licensed. Nevertheless, only 55 % of tocilizumab-treated patients in the GIACTA trial had sustained glucocorticoid-free remission at 52 weeks [4], with large vessel vasculitis persisting in some patients despite treatment [5]. This highlights the need for alternative therapeutic strategies. Greater understanding of molecular pathogenesis and patient heterogeneity is needed to develop therapies that improve the management of GCA in line with other autoimmune diseases, including precision medicine strategies.

Current understanding of GCA pathogenesis stems from histopathological analyses of temporal artery biopsies (TAB) which demonstrate infiltration of the arterial wall by lymphocytes and monocytes that enter through networks of new blood vessels (neoangiogenesis). The characteristic granulomatous infiltrate is primarily comprised primarily of $CD4^+$ T-cells and macrophages. Other immune cells are present in lower frequency, including $CD8^+$ T-cells, tissue resident memory T-cells, B cells and plasma cells. Thickening of the arterial intima, leading to luminal occlusion and ischaemic tissue injury, is a key pathological response to inflammation, which is associated with vascular wall injury and myofibroblast proliferation [6–8].

International genetic studies support a significant role for T-cells. There is a strong major histocompatibility complex (MHC) association, with multiple independent genetic effects including *HLA-DRB1*, *HLA-DQA1* and *HLA-B*. Several loci involved in polarization of T-cells towards Th1, Th17 or Treg phenotypes were identified at sub-GWAS significance, e.g. *IL6*, *TNF*, *IL17A*, *IL12* and *PTPN22* [9–11]. It remains debated whether T-cell accumulation in the vessel wall occurs due to the presence of a vascular auto or neoantigen, chronic infection or non-specific recruitment to an inflamed tissue due to defects in an immune checkpoint [12–14]. This distinction is important and may guide disease management, since persistence of an autoreactive T-cell clone may require long-term immunosuppression to prevent progressive vascular damage. The "Holy Grail" in this scenario would be therapeutic strategies that reinduce immunological tolerance and immune privilege within the vessel wall.

Detailed study of T-cell receptor (TCR) repertoires in GCA may help determine whether the observed T-cell infiltrate is a bystander effect or an (auto/neo) antigen-driven process. Early molecular studies, using Sanger sequencing, revealed expansions of some TCR Vβ families in TAB, suggestive of an antigen-specific response [15–17]. In one study, 2/3 patients shared an expansion in Vβ5.3. Both patients carried the HLA-DRB1*0401 allele, supportive of a common MHC class II presented (auto/neo) antigen [15]. In an elegant xenotransplantation model, adoptive transfer of T-cells from arterial lesions, but not blood, reconstituted the IL-2 and IFNγ transcriptional signature in SCID mice, providing evidence for enrichment of antigen-specific T-cells within arterial lesions [18].

Here, we employed next generation sequencing technologies to enable detailed analysis of TCRβ-chain rearrangements in peripheral blood and TAB from GCA patients and controls. Using amino acid sequence similarity-based clustering, we aimed to identify TCR rearrangements that were consistently associated with GCA, identify their sequence patterns and associations with clinical and histological variables.

2. Material and methods

2.1. Study cohorts

All samples were obtained with written, informed consent, following the Declaration of Helsinki. We recruited 72 subjects from the UK GCA Consortium, with GCA clinical diagnosis confirmed by a rheumatologist or ophthalmologist, and with a TAB and/or blood sample available within 4 months of diagnosis. All patients were treated with 40–60 mg prednisolone at presentation, and none were treated with disease-modifying antirheumatic drugs at the time of sample collection. We retrospectively applied the 2022 ACR criteria for GCA to our cohort [2,19]. Ethical approval was granted by the Yorkshire and Humber–Leeds West Research Ethics Committee (05/Q1108/28).

69 "non-inflammatory" controls were recruited from University of Leeds staff and a cataract pre-assessment clinic (paroxysmal nocturnal haemoglobinuria (PNH) Research Tissue Bank 16/YH/0290 and Leeds East Research Ethics Committee 04/Q1206/107, respectively). An existing genomic DNA TCRβ dataset from 39 PNH and 33 aplastic anaemia patients from the PNH research tissue bank was used as "disease" controls.

2.2. HLA genotyping, quality control and imputation

Genotypic data from one of two versions of the Illumina infinium Human core 24 Beadchip (HumanCore-12v1-0_A) were available from 55 GCA cases [9,10]. As a post-quality control filter, we removed variants with a minor allele frequency (MAF) < 0.01 and variants with an information score <0.8. Classical HLA alleles were imputed from SNP genotyping results across the extended major histocompatibility complex (MHC) using the SNP2HLA imputation method [20]. Associations with SNPs (rs9268969, rs477515) and HLA-DRB1*04, previously associated with biopsy-confirmed GCA, were determined [9,10].

2.3. T-cell receptor sequencing

Genomic DNA was extracted from peripheral blood samples and formalin-fixed paraffin embedded (FFPE) TAB retrieved from pathology archives. Briefly, FFPE blocks were pre-chilled overnight at 4 °C, placed on ice with dH_2O, and sectioned (20–30 × 5 mm) using a LEICA RM 2125RTF microtome. Following deparaffinization, genomic DNA was extracted using the QIAmp DNA FFPE Tissue kit, according to the manufacturer's protocol and eluted in 25 ml of Buffer ATE. DNA quantification was performed using DeNovix DS-11 or NanoDrop.

200 ng of DNA was used for each 20 μ l PCR reaction that comprised a denaturation, 35 amplification and a final extension cycle, using a modification of established protocols which added linker sequences to standard BIOMED-2 primers [21,22]. Two reactions were performed for each sample, whereby the J primers were separated out to prevent non-specific interactions [23]. The 2 reactions were combined for purification and PCR clean-up was performed using Pronex® Size-Selective Purification System (Promega). Samples were stored overnight at 4 °C. Nextera XT Indexes (Illumina, Nextera XT Index Kit v2 Set A) were incorporated in a 20 μ l PCR reaction and samples were run on a 2 % GTG agarose gel until good band separation was observed. Bands of approximately 376–433bp were cut out using a fresh scalpel blade and purified using Zymoclean™ Gel DNA Recovery Kit (Zymoresearch), according to the manufacturer's protocol. Agilent D1000 ScreenTape (Agilent) was used to check DNA quality on the Agilent 4150 Tapestation System. A peak between 376 and 433bp was observed for each sample. Quant-iT™ PicoGreen™ dsDNA Assay Kit (ThermoFisher) was used to quantify the final libraries and plate was read on the FluoStar fluorimeter to calculate DNA concentrations. 8 ng of each FFPE sample and 10 ng of each DNA sample was added to the final pool, ensuring no more than 7 μ l of any sample was used to avoid skewing. Sequencing was performed on a MiSeq (Illumina) using 2 × 250bp kit.

Raw TCR sequencing data were preprocessed using MiXCR [24,25], combining forward and reverse sequencing runs using the international immunogenetics information system (IMGT) library [26]. Clones were defined by shared V gene and complementary-determining region 3 (CDR3) sequence, with nonfunctional clones discarded. Over 85 % of aligned sequences were retained. To remove sequencing errors,

sequences with fewer than 3 reads were discarded. Sequences with fewer than 10 reads were removed if another sequence in the sample had only one nucleotide difference in the CDR3 sequence. A recognised source of errors in TCR sequencing is DNA contamination, where tiny amounts of DNA get transported from one sample to the next [27]. To address contamination, identical CDR3 sequences were examined across different patients. If a clone was >10 times more expanded in one sample compared to others, the low-expansion occurrences were considered contamination and removed.

2.4. Computational analyses

2.4.1. Diversity

Repertoire diversity was assessed using the Hill numbers, specialized diversity measures that balance species count and population evenness. Namely, species richness measures the number of species in the sample. Shannon diversity quantifies the uncertainty in predicting the type of a randomly picked sample. Combining these diversity indices gives a comprehensive overview of TCR species distribution within samples [28].

2.4.2. TCR classification

To identify GCA-associated TCRs in peripheral blood DNA, we sought to identify TCRs that our clustering algorithm consistently identified as coming from GCA patients, focusing on TCR sequences with at least 10 reads to eliminate unexpanded, naive T-cells.

For independent analyses, we randomly sampled 10,000 TCRs each from the GCA group and the control group. We calculated all TCR pairwise distances using the well-established tcrdist3 distance, which considers V and J segment similarity and CDR3 sequence edit distance, effective for clustering TCRs by epitope specificity [29]. Distances over 100 were ignored to prioritize close neighbours.

Data were divided into 5 cross-validation folds, keeping TCRs from the same subject in the same fold to prevent potential misclassification as GCA-specific due to similarity to other TCRs from the same individual. A K-nearest neighbour (K-NN) classifier was trained on four folds and evaluated on the remaining fold. The classifier should not be expected to identify all GCA TCRs, as most TCRs in GCA patients are likely unrelated to the disease, with only a small subset of TCRs likely being involved in GCA pathogenesis. This setup corresponds to a weak label setting, and the goal of the model is to identify a small number of consistently GCA-associated TCRs. The analysis was repeated 500 times to infer a frequency distribution of correctly identified GCA TCRs (true positives).

The predictive model performance was assessed using various scores based on true positives, false positives, true negatives, and false negatives. From these, the following performance scores were derived:

$$Accuracy = (\text{true positive} + \text{true negative}) / (\text{true positive} + \text{true negative} + \text{false positive} + \text{false negative})$$

$$Sensitivity = \text{true positive}/(\text{true positive} + \text{false negative})$$

$$Specificity = \text{true negative}/(\text{true negative} + \text{false negative})$$

A perfect model should score 1 on all performance metrics, however, in our weak label setting, we expect moderate accuracy and sensitivity for individual TCRs, hence our focus on predicting GCA-associated TCRs rather than causally linked TCRs.

2.4.3. Hyperparameter comparison

We optimized two hyperparameters: the number of neighbours "*k*" used by the K-NN classifier and the probability cutoff "*t*" to classify a TCR as GCA-specific. The K-NN classifier predicts the probability of a test sample belonging to a GCA patient by averaging the labels of the *k* most similar samples (i.e. neighbours) in the training set. We use the probability cutoff *t* to decide when to classify a test sample as GCA-specific, based on the output of the K-NN classifier. For example, with *t=0.5* every sample with a prediction *>0.5* would be classified as GCA-specific.

Higher *k* reduces noise but may miss smaller TCR clusters. High *t* emphasizes individual experiments, while low *t* favours the ensemble of 500 experiments. We analysed all combinations of k = 3, 5, 7, 11, 15, 19 and t = 0.5, 0.65, 0.75, 0.85, totalling 24 hyperparameter settings [30]. To assess the consistency of the results across hyperparameter settings, we compared the ranks of the 1000 TCRs most consistently identified as true positive across 500 experiments with the same hyperparameters. Ranks were compared using the normalized discounted cumulative gain (nDCG) score [31].

2.4.4. TCR clustering

TCR clusters were identified using a graph-based approach. Namely, to identify clusters, we used all GCA-associated TCRs as nodes and calculated pairwise distances using the tcrdist3 metric, including TCRs from both GCA patients and control subjects to identify their nearest neighbours. A graph was constructed where TCRs were connected by edges if they were among each other's 19 nearest neighbours. Community detection was then performed using the Girvan–Newman method [32]. TCRs that did not belong to any community (i.e., not within the 19 nearest neighbours of any other GCA-associated TCRs) were assigned a cluster label of 0.

2.4.5. Identification of similar TCRs in VDJ database

The VDJ database (VDJdb) [33] was downloaded on August 13th, 2024. Only human TCRβ sequences with a confidence score of at least 1 were retained. Since no direct matches of GCA-associated TCRs were found, we considered sequences with one amino acid difference in the CDR3 region as matches.

2.5. Statistical analyses

Distributions are reported as median ± interquartile range. All P values were calculated using the Mann-Whitney-U test. Subjects with missing data were excluded only from the specific comparison, not from all analyses. For clinical associations, we computed the expansion of GCA-associated TCRs in peripheral blood, representing the fraction of the repertoire made up of GCA-associated TCRs.

3. Results

3.1. Cohort description

The GCA patients were representative of secondary care populations from the UK; 71 (99 %) were White European, 51 (71 %) were female with a median (± interquartile range) age of 72 (±9) years. In 53 (73 %) the diagnosis was confirmed by a positive TAB or medical imaging and 64 (89 %) retrospectively fulfilled the 2022 ACR classification criteria for GCA [19]. For the 19 subjects where the diagnosis was not confirmed by TAB, 13 (68 %) fulfilled the 2022 criteria, 5 did not and it was

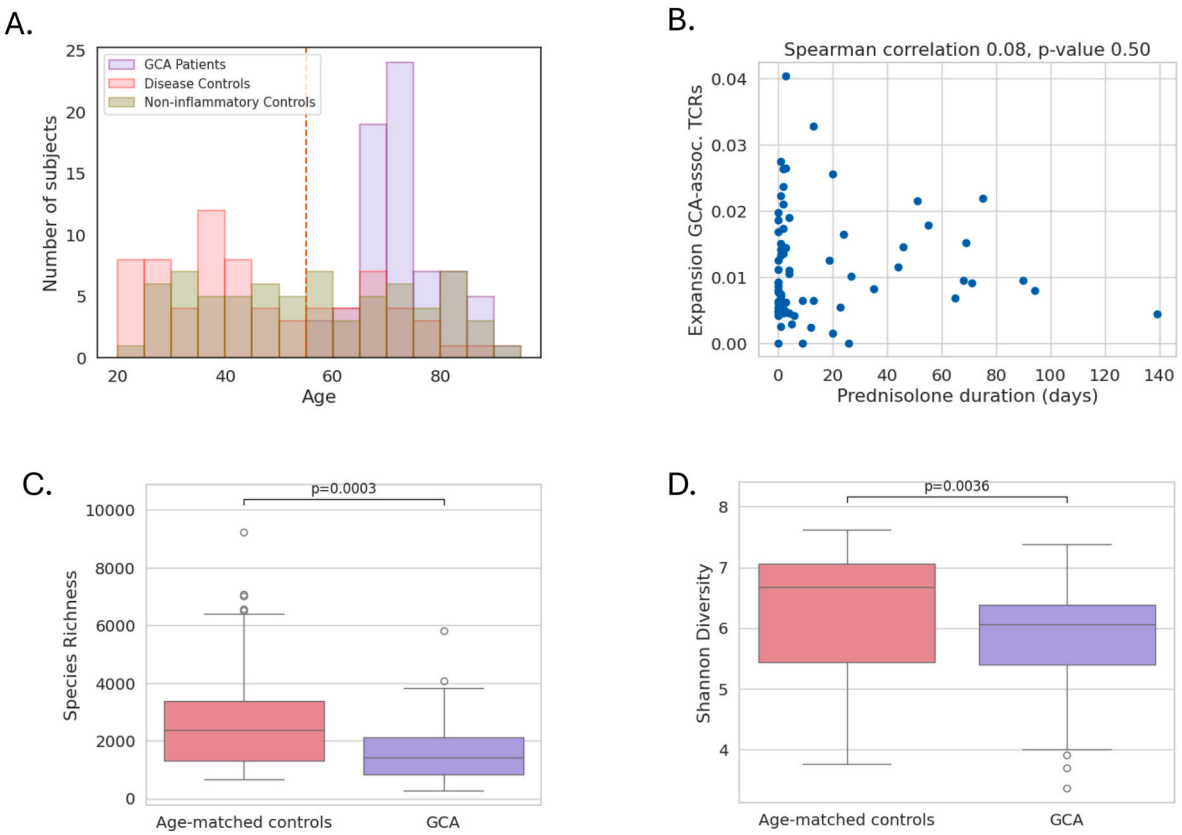

Fig. 1. Dataset overview and repertoire diversity. A) The cohort consisted of 72 giant cell arteritis (GCA) patients, 72 "disease" controls, and 69 "non-inflammatory" controls. GCA patients with a median age of 72 ± 9 years were significantly older than the control subjects with a median age of 48 ± 31 ($P < 0.001$). The orange vertical line highlights the age-matched control group, whereby all control subjects over 55 years ($n = 60$) were retained from both control groups, with a median age of 69.5 ± 15.5 years, which matched the GCA age distribution ($P = 0.13$). B) There was no evidence that the GCA-associated T-cell receptor (TCR) expansion was associated with the duration of prednisolone therapy prior to peripheral blood sample collection (Spearman correlation 0.08, $P = 0.50$). C) The species richness observed in TCR repertoires of GCA patients was significantly lower when compared to age-matched controls ($P = 0.0003$). D) Shannon diversity in TCR repertoires of GCA patients was significantly lower compared to age-matched controls ($P = 0.0036$). (*: $P < 0.05$, **: $P < 0.01$, ***: $P < 0.001$). (For interpretation of the references to colour in this figure legend, the reader is referred to the Web version of this article.)

unknown for 1 individual. A variety of clinical phenotypes were represented, 29 (40 %) had concomitant polymyalgic symptoms or polymyalgia rheumatica (PMR) and 9 (12.5 %) had cranial ischaemic complications at presentation (permanent visual loss, stroke, cranial neuropathies or scalp necrosis), with an additional 44 (61 %) experiencing transient cranial ischaemic features at presentation (jaw/tongue claudication, visual disturbance, diplopia, transient ischaemic attack, etc.).

GCA patients were older than combined non-inflammatory and disease control subjects ($P < 0.001$; Fig. 1A). To exclude the influence of age in our analyses, we constructed an age-matched control dataset, by retaining 60 subjects over 55 years (35 non-inflammatory and 24 disease controls), with no residual age difference ($P = 0.13$) with a median age of 69.5 ± 15.5 years. However, non-inflammatory age-matched controls (median age 71.5 ± 17.25) remained older than disease controls (median age 66.0± 10.5), although in control individuals under 70 Shannon diversity and species richness were not unduly influenced by the type of control cohort (Supplementary Fig. 1). Further analysis of the reduced non-inflammatory control dataset was used to investigate the influence of disease controls.

After the described preprocessing, we obtained 67,062 unique TCRs from the peripheral blood of GCA patients, 41,750 from the non-inflammatory age-matched controls, and 30,425 from the age-matched disease controls. Additionally, we analysed the TAB TCR repertoires of 30 GCA patients, 27 of whom had a positive biopsy. Most GCA patients received prednisolone prior to sample collection and the median duration of steroid treatment was 5 (±4) days for TAB and 3 (±19.5) days for peripheral blood. There was no correlation between the duration of prednisolone treatment and expansion of GCA-associated TCRs (Spearman correlation 0.08, $P = 0.50$; Fig. 1B).

3.2. Repertoire diversity and clonality

Antigen-specific T-cell responses result in clonal expansions of selected TCRs. The extent of the expansions can be captured with repertoire diversity measures, such as species richness and Shannon diversity [34][. Since age can have a significant influence on the TCR repertoire [35], we used an age-matched control cohort for the diversity comparisons. We observed that species richness and Shannon diversity were significantly lower ($P = 0.0003$ and $P = 0.004$, respectively) in GCA patient peripheral blood TCR repertoires compared to the age-matched controls (Fig. 1C and D, respectively). This suggested that GCA patients had more T-cell clonal expansions.

3.3. Identification of GCA-associated TCRs

We hypothesized that GCA-related TCRs were more similar to each other than background TCRs from controls and could be identified across GCA patients using a similarity-based classification algorithm.

We applied a K-NN classifier based on tcrdist3, an established TCR similarity metric, to predict which TCR sequences in the test set were more likely to have stemmed from GCA patients, summarised in Fig. 2A.

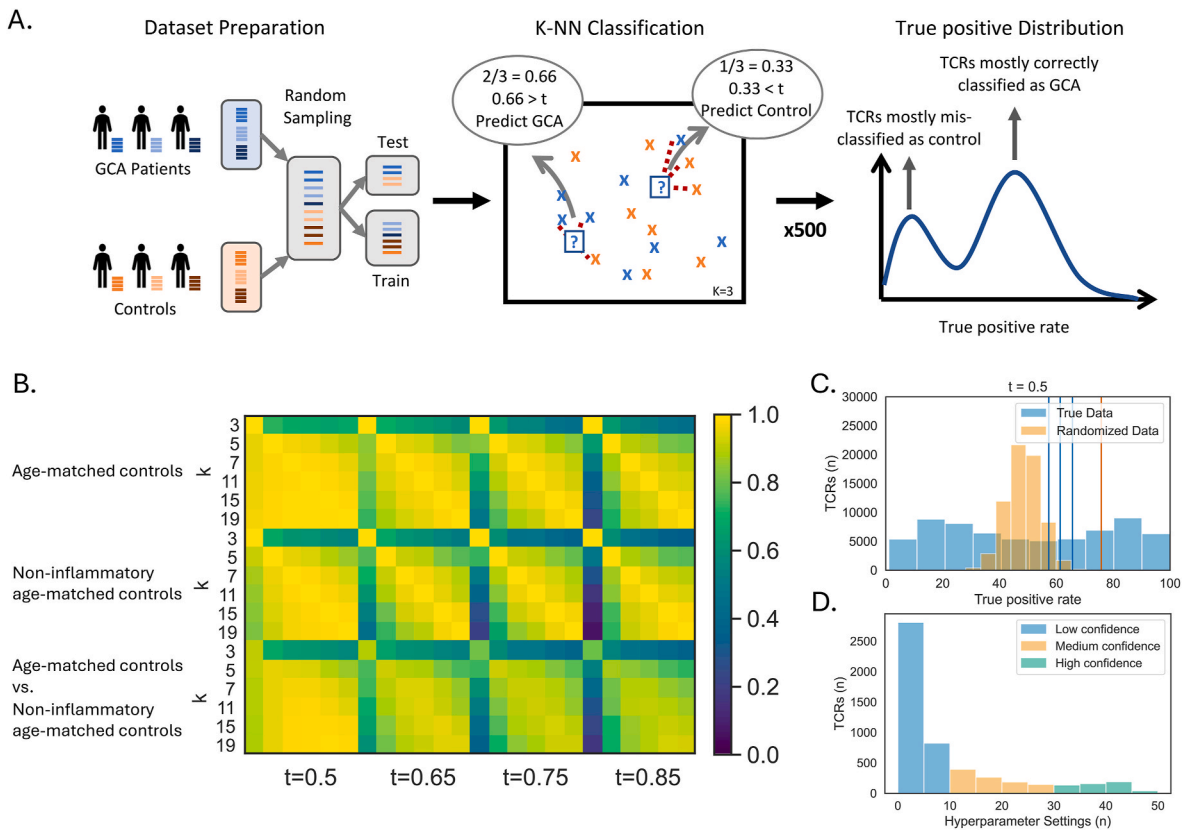

Fig. 2. K-nearest-neighbour (K-NN) classification. A) Visualization of experimental methods. We collected T-cell receptor (TCR) repertoire data from giant cell arteritis (GCA) and control subjects. From these, we randomly sampled 10,000 positive (i.e. GCA) and 10,000 negative (i.e. control) sequences. We performed patient-wise five-fold cross validation and classified the validation sequences using a K-NN classifier. By repeating the experiment 500 times, we obtained a distribution of how often each positive TCR has been correctly classified (true positive rate). B) Normalized discounted cumulative gain (nDCG) score of agreement among the top 1000 TCRs using the age-matched control group and different hyperparameter settings. All hyperparameter settings have a good agreement with each other (median nDCG = 0.94 ± 0.16), with the exception of $k = 3$, which tended to have poor agreement with settings with $k > 10$. nDCG score of agreement among the top 1000 TCRs using the non-inflammatory age-matched control group and different hyperparameter settings. Again, all hyperparameter settings had good agreement with each other (median nDCG = 0.91 ± 0.22), with reduced agreement for $k = 3$. C) Distribution of true positive classifications in experiment using the age-matched control group, *k=11* and *t=0.5* for data with true and randomized labels. In the random setting, we observed a gaussian distribution around 50 %, as expected for 50 % positive labels and a cutoff *t* of 0.5. In the true data we observed a bimodal distribution, with TCRs classified as true positive far more or far less often than expected randomly. Blue lines show significance levels of 0.05, 0.01 and 0.001, red line show the highest value observed in the random distribution. D) Distribution of number of times a TCR appeared among the top 1000 sequences in any of the 48 settings. TCRs that were consistently identified as GCA-specific in more than 30 hyperparameter settings got a high confidence score (green), those identified in 10–30 settings got a medium confidence score (orange), all others got a low confidence score (blue). (For interpretation of the references to colour in this figure legend, the reader is referred to the Web version of this article.)

The K-NN classifier predicted the label (GCA or control) of a given TCR in the test set based on the labels of its *k* nearest neighbours in the training set. If clusters of similar TCRs co-existed in GCA patients and were not observed in controls, these would be consistently identified as GCA-specific across multiple repeats of the analysis. The percentage of times a TCR was correctly identified as stemming from a GCA patient (true positive rate) served as a measure of how strongly a specific TCR sequence was associated with GCA.

We performed sensitivity analyses to investigate the effect of age and inclusion of disease controls. Analysis of TCR repertoires from all controls in the classification biased our results towards the detection of age-specific rather than GCA-specific TCRs, and hence, we defined an age-matched control group. The effect of additionally excluding disease controls was marginal, as the 1000 TCRs with the highest true positive rate had a high agreement with each other (median nDCG score = 0.92 ± 0.03 across all combinations of hyperparameter settings).

To assess consistency, we repeated the classification procedure for all combinations of the hyperparameters *k=3, 5, 9, 11, 15, 19* and *t=0.5 0.65, 0.75, 0.85*. Fig. 2B shows that with both age-matched controls and non-inflammatory age-matched controls, there was a high agreement between the 1000 TCRs with the highest true positive rate across all hyperparameter settings (median nDCG score = 0.94 ± 0.16 and 0.91 ± 0.22, respectively). For k < 5, consistency was reduced due to a higher level of noise in the predictions.

To estimate the statistical significance of our results, we applied a bootstrapping approach, where we repeated the analysis using randomly shuffled GCA and control status (null hypothesis). Fig. 2C shows the true positive rate distributions for one example using the age-matched control group and hyperparameter settings $k = 11$ and $t = 0.5$ for the true and randomized data. There was a large shift in the distribution of true positive rates in the true compared to the randomized data, with peaks both at lower and higher true positive rates than observed in the randomized data ($P < 0.001$). This matched our expectations, as we operated in a weak label setting. We expected only a subset of TCRs from GCA patients to be involved in the disease process, while the rest were non-GCA associated TCRs, i.e. false positives. We found that generally more than 10,000 TCRs were found in the right-hand tail of the distribution, fully outside of the random distribution.

3.4. Identification of TCR sequence similarities in giant cell arteritis

For further analyses, we aimed to retain only TCRs that were most

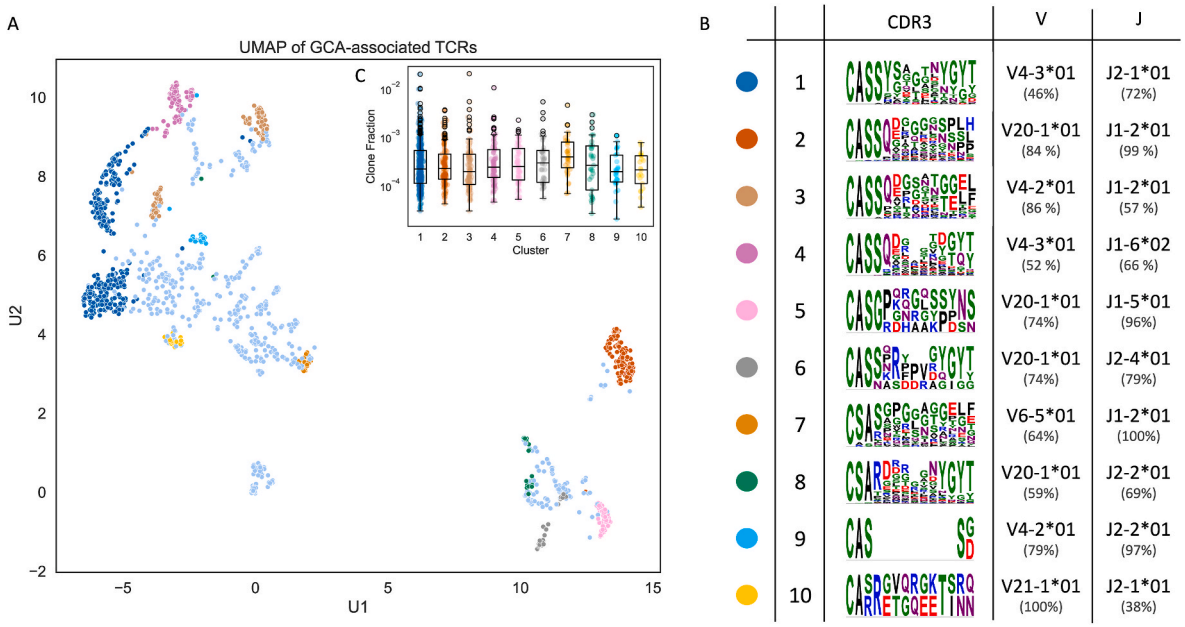

Fig. 3. ***Clustering of giant cell arteritis-associated T-cell receptors.*** A) Sequence similarities between all 1526 giant cell arteritis (GCA)-associated T-cell receptors (TCRs) visualized on a Uniform Manifold Approximation and Projection (UMAP) plot of the tcrdist3 distances. Colours correspond to communities in the K-nearest-neighbour graph (*k=19*), with light blue denoting TCRs not fitted into any cluster. B) TCR clusters corresponded to specific regions in the UMAP space and were mostly defined by a clear sequence pattern seen in the sequence logo of the complementarity-determining region 3 (CDR3) region. Columns show the most used V and J segment in each cluster, with their percentages. C) Expansion of TCRs per cluster. The average expansion was low, making up 0.001 %–0.01 % of a patient's peripheral repertoire. Cluster 7 showed a slightly higher median expansion compared to the other clusters. The center of the boxplot marks the sample median, and the box extends from lower to upper quartile. (For interpretation of the references to colour in this figure legend, the reader is referred to the Web version of this article.)

likely to be associated with GCA. We deployed an ensemble strategy and checked how often each TCR occurred in the top 1000 TCRs with the highest true positive rate across all 48 parameter settings. The distribution is shown in Fig. 2D. Based on these results, we assigned each TCR a low, medium or high confidence score (low confidence: among top 1000 in <10 hyperparameter settings, medium confidence: among top 1000 in 10–30 hyperparameter settings, high confidence: among top 1000 in >30 hyperparameter settings). This provided us with a set of 1526 unique TCRs with high or medium confidence scores, which were consistently associated with GCA across multiple model hyperparameters and experimental replicates.

To find and visualize GCA-specific TCR sequence patterns, we clustered the 1526 unique TCR these TCR sequences using the tcrdist3 distance measure (Section 2.3.5). Fig. 3A visualizes the GCA-associated TCRs on a Uniform Manifold Approximation and Projection (UMAP) plot. All clusters with more than 15 sequences are shown in Fig. 3B along with the sequence logo of the CDR3 sequence, as well as the most used V and J segments. Whilst only 57 % of GCA-associated TCRs could be fitted into a cluster, the clusters that were observed corresponded to defined regions in the UMAP and often showed distinct sequence patterns and common TCR V and J segment usage.

Analysis of peripheral blood provides a snapshot of cells transiting between the lymph nodes and tissues and is not necessarily reflective of the total pool of autoreactive cells. GCA-associated TCRs tended to display low expansions in peripheral blood, making up between 0.001 % and 0.01 % of a patient's repertoire (Fig. 3C). A slightly higher expansion was observed for TCRs in cluster 7.

Within the GCA-associated TCRs, several V and J segments were overrepresented in comparison to all control repertoires (Fig. 4). In particular, the TRBV20-1*01, TRBV4-3*01, TRBV4-2*01 and TRBV4-1*01 segments occurred at least 10 % more often among the GCA-associated TCRs than in control repertoires. The largest difference was seen for TRBJ1-2*01, which occurred more than 30 % more often in GCA-associated TCRs than in control repertoires.

3.5. Identification of potential giant cell arteritis autoantigens

While the observed sequence patterns suggest a common antigen, to date, the options to identify potential antigens directly from TCRβ sequencing are severely limited. The largest database to collect TCR specificities, VDJdb [33], can be used to check whether a certain TCR already has an experimentally verified target recorded (mammalian or microbial). However, the VDJdb is heavily biased towards viral antigens and contains only 633 TCRs with human epitopes, which are mainly cancer neoantigens. While none of the identified GCA-associated TCRs has so far been recorded in VDJdb, 27/1526 receptors had a counterpart in VDJdb that differed by only one amino acid in the CDR3 sequence and did not have a low confidence score. Of these, five have been shown to bind human proteins, five were associated with CMV, five with MCPyV, six bind HIV-1 epitopes and the other six were specific for other viral epitopes. The identified matches with epitopes of human origin are listed in Table 1. Note that for three out of the five identified matches, the associated HLA type matched one of the known GCA HLA associations in *HLA-DRB1*, *HLA-DQA1 or HLA-B*. Moreover, all the TCRs with matches with human epitopes in VDJdb belonged to cluster 1, while only 20 % of all GCA-associated TCRs fell into cluster 1.

3.6. Clinical and histological associations

We explored whether expansion of GCA-associated TCRs in peripheral blood repertoires correlated with clinical phenotypes (Fig. 5A–C). We observed that GCA patients with a positive TAB had significantly higher expansions of GCA-associated TCRs in blood compared to patients with a clinical diagnosis (Fig. 5A, P = 0.014). There was no association between GCA-associated TCR expansion and potential confounding factors such as age, sex and number of days between diagnosis and blood sample collection, equating to duration of steroid therapy. Nor was there an association with polymyalgic symptoms or PMR or the presence of cranial ischaemic complications at diagnosis

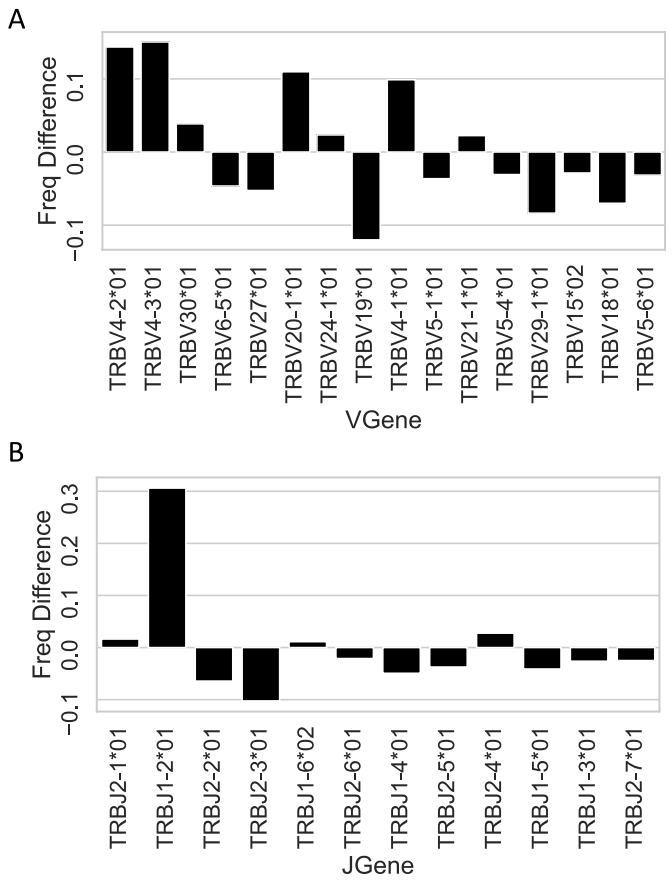

Fig. 4. TRBV and TRBJ segment usage in giant cell arteritis-associated T-cell receptors. A) Comparing the V segment usage of giant cell arteritis (GCA)-associated T-cell receptors (TCRs) to the distribution observed in all control repertoires showed increased usage of the V segments TRBV20-1*01, TRBV4-3*01, TRBV4-2*01 and TRBV4-1*01. B) The usage of J segment TRBJ1-2*01 was increased by 30 % in GCA-associated TCRs compared to all control repertoires.

(Fig. 5B and C).

There was no association between HLA-DRB1*04 nor GCA-associated SNPs (rs9268969 and rs477515) and the expansion of GCA-associated TCRs in peripheral blood (see Fig. 5D–F, respectively).

Of the 1526 GCA-associated TCRs identified in peripheral blood, 63 were also detected in TAB repertoires from the 30 cases with paired samples. Identical GCA-associated TCRs were observed in both blood and tissue samples from 21/30 GCA cases. None of these TCR sequences overlapped with the human antigenic epitopes shown in Table 1, nor any mammalian or microbial species in the public domain.

4. Discussion

In this study we detected clonal T-cell expansions in the peripheral blood of GCA patients compared with age-matched controls through the analysis of TCR repertoire diversity. We found a set of 1526 TCRs that were consistently associated with GCA with high or medium confidence according to a K-NN classifier across multiple model parameters and experimental replicates. These TCRs made up 0.001–0.01 % of the peripheral repertoire, suggestive of T-cell clonal expansion but not hyper-expansion as observed with CMV. We employed TCR sequence clustering algorithms and fitted 57 % of GCA-specific TCRs into 10 clusters, which displayed distinct TCR sequences and TCR V and J segment usage. Over-representation of TRBV20-1*01, TRBV4-3*01, TRBV4-2*01 and TRBV4-1*01 segments was observed. These TCR V segments occurred at least 10 % more often among GCA patients than in controls. The largest overrepresentation was seen for TRBJ1-2*01, which was over-represented by more than 30 % in GCA repertoires. The absence of TRB11 suggests these expansions were not type 1 NK T-cells. There was no association with HLA-DRB1*04, nor GCA-associated SNPs within the MHC.

Clustering of GCA cases in space and time is suggestive of an environmental trigger in genetically susceptible individuals with most studies to date exploring infectious triggers [36–38]. Putative organisms proposed include parvovirus B19, human parainfluenza type 1 virus, respiratory syncytial virus, adenovirus, Epstein Barr virus (EBV), varicella-zoster virus, *Mycoplasma pneumoniae* and *Chlamydia pneumoniae* [39–47]. However, case-control studies have not produced conclusive evidence for a single infectious trigger. To explore whether a subset of the identified GCA-associated TCRs could potentially be associated with infectious rather than GCA-specific antigens, we exploited 11,016 TCR sequences from the largest public database (VDJdb), which is heavily biased towards viral antigens. None of the 1526 GCA-associated TCRs were recorded in VDJdb, however, we identified 27 TCRs that differed by only one amino acid in the CDR3 sequence, which were specific for viruses, including human immunodeficiency virus 1, cytomegalovirus and Merkel cell polyomavirus. Nevertheless, VDJdb only contained antigens from one of the previously reported infectious agents, EBV, and only one of the 1073 EBV-binding TCRs found in VDJdb was similar to one of our identified GCA-associated TCRs, suggesting EBV is unlikely to be a significant GCA trigger in most patients.

Higher GCA-associated TCR expansions were observed in patients with a positive TAB, but there was no association with cranial ischaemic complications nor PMR, suggesting these expansions were associated with GCA pathogenesis, rather than the disease phenotype.

We then interrogated the VDJdb for TCR sequences to known human epitopes. Unfortunately, only 619 were recorded, to date, which were mainly cancer neoantigens with no matches to our TCR sequences. However, we identified 4 TCR sequences that differed by one amino acid and that were reported to bind human proteins (ATP-dependent DNA helicase Q5, glucosidase II alpha subunit, Triosephosphate Isomerase 1, and Melanoma-associated antigen 6) and another synthetic insulin. All 4 proteins are observed in arterial tissue, in public databases, albeit at low levels for Melanoma-associated antigen 6. As TCR databases continue to expand to include more human proteins, there is the possibility that more GCA-associated antigens may be identified from this dataset, which has been made publicly available.

The novel technologies and analytical approaches applied in this study, were those suitable for use on archived samples in rare diseases, such as peripheral blood and tissue DNA. This allowed relatively large

Table 1
Identification of potential human GCA-antigenic epitopes from VDJdb.

Gene	Epitope	MHC A	MHC B	CDR3	VDJdb Score	Cluster
RECQL5	GEEDGAGGHSL	HLA-B*44:02	B2M	CASSQAGGTGELFF	2	1
GANAB	ALYGFVPVL	HLA-A*02:01	B2M	CASSQGGDEQFF	2	1
TPI1	GELIGILNAAKVPAD	HLA-DRA*01:01:02	HLA-DRB1*01:01:01	CASSQIRETQYF	3	1
Synthetic hybrid insulin	GQVELGGGNAVEVCKGS	HLA-DQA1*03:01	HLA-DQB1*03:02	CASSLERETQYF	3	1
MAGEA6	KVDPIGHVY	HLA-A*01:01	B2M	CASSFDRGYGYTF	2	1

CDR3: complementarity-determining region 3; MHC: major histocompatibility complex.

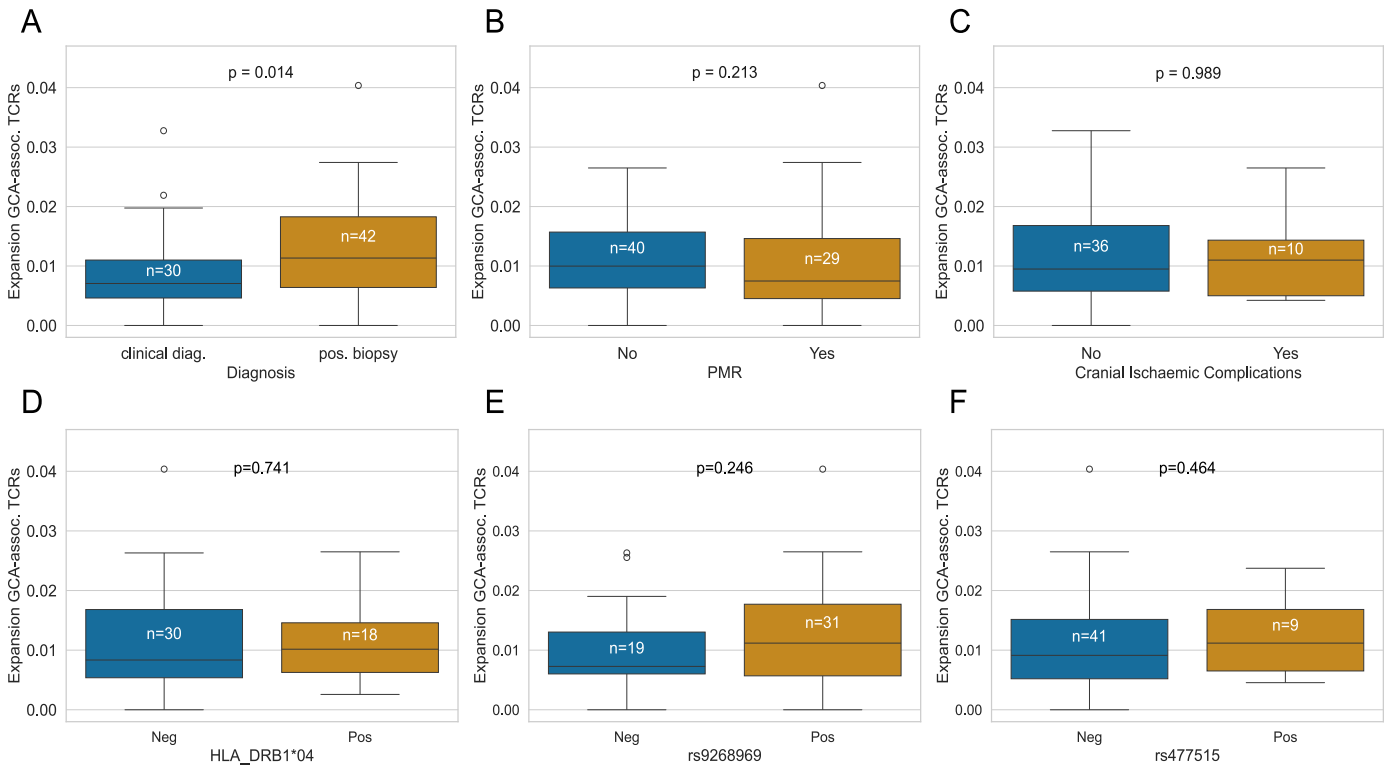

Fig. 5. T-cell receptor association with clinical and histological features. A) Patients with a positive temporal artery biopsy (TAB) exhibited a significantly higher expansion of GCA-associated T-cell receptors (TCRs) in the peripheral repertoire compared to patients with only a clinical diagnosis of giant cell arteritis (GCA) (P = 0.014). B) and C) The occurrence of polymyalgic symptoms or a polymyalgia rheumatica (PMR) -diagnosis and cranial ischaemic complications, respectively, were not significantly influenced by the expansion of GCA-associated TCRs in blood. D-F) The GCA-associated HLA type HLA-DRB1*04 and SNPs rs9268969 and rs477515, respectively, were not associated with expansion of GCA-associated TCRs in the peripheral repertoire. All boxplots: the center of the boxplot marks the sample median, and the box extends from lower to upper quartile.

numbers of T-cells, cases and controls to be studied. The disadvantages of this approach are that clonal expansions cannot be attributed to a specific T-cell subset, including $CD4^+$ or $CD8^+$ T-cells. Furthermore, the full TCR, including both alpha and beta chains cannot be reconstructed. Single cell methodologies offer much promise but are dependent on prospective sample collection, which is logistically difficult in rare diseases, and current costs preclude exploration of large numbers of T-cells in sufficient cases and controls to detect rare clonal expansions.

5. Conclusion

Our data support ongoing evaluation of therapeutically targeting T-cells in GCA, with early phase clinical trials showing promising results for abatacept [48] and baricitinib [49]. Abatacept comprises the extracellular domain of CTLA4 fused to the IgG1 Fc, thus blocking the second T-cell activation signal. Baricitinib is a Janus Kinase inhibitor which suppress intracellular signalling downstream of cytokines and growth factors which downregulates cytokine induced T-cell differentiation and polarization, amongst other biological effects.

It is possible that different biological pathways dominate in different patients and access to biomarkers that identify patients with a T-cell dominant disease may improve the success rate of these treatments. Further studies exploring TCR repertoires, including persistence in the circulation and expansion during relapse will determine if patient/GCA-specific TCR may provide such molecular biomarkers.

CRediT authorship contribution statement

Anna Weber: Writing – original draft, Formal analysis, Data curation. **Michal Zulcinski:** Writing – review & editing, Formal analysis, Data curation. **Lubna Haroon-Rashid:** Writing – review & editing, Methodology, Investigation. **Beth Kuszlewicz:** Writing – review & editing, Methodology. **Alice Driessen:** Writing – review & editing, Supervision. **Darren Newton:** Writing – review & editing, Supervision, Resources, Funding acquisition, Data curation, Conceptualization. **Ann W. Morgan:** Writing – review & editing, Supervision, Resources, Funding acquisition, Data curation, Conceptualization. **María Rodríguez Martínez:** Writing – review & editing, Supervision, Methodology, Conceptualization.

Data statement

T-cell receptor repertoires will be made available under:
DOI: 10.5281/zenodo.14261345.
For data protection reasons no patient metadata or clinical variables will be made available.
Code for the bioinformatics analyses is available under:
DOI: 10.5281/zenodo.14269839.

Funding sources

This work was supported in part by the HELICAL Innovative Training Network, a European Commission funded project under the Horizon 2020 research and innovation programme under the Marie Skłodowska-Curie (813545 and 955321); Horizon 2020 ICT-2018-2 Program (826121); Swiss National Science Foundation (Sinergia program CRSII5_193832 and Project Funding 200021_192128); Medical Research Council (MRC) TARGET Partnership grant (MR/N011775/1), National Institute for Health and Social Care Research (NIHR) Leeds BRC (IS_BRC_1215_20015, NIHR203331), University of Leeds Anniversary PhD studentship and an NIHR Senior Investigator Award to Morgan (NIHR202395). The funders had no input in relation to the study design,

collection, analysis and interpretation of data, writing of the manuscript or decision to submit the article for publication.

This study was supported in part by the NIHR Leeds BRC. The views expressed are those of the authors and not necessarily those of the NIHR or the Department of Health and Social Care.

Declaration of competing interest

Morgan reports: consultancy fees payable to her institution from Roche/Chugai, Sanofi/Regeneron, Glaxo Smith Kline and AstraZeneca, outside the submitted work. Reports research and/or educational funding were received from Roche/Chugai and Kiniksa Pharmaceuticals, outside the submitted work. The remaining authors declare no competing interests.

Acknowledgements

We thank all patients who generously contributed to this research, clinical and nursing staff who supported patient recruitment, in particular Dr Sarah Mackie. We also thank Dr Louise Sorenson the UK GCA Consortium project manager for her work in co-ordinating this study and subsequent data collection and validation.

Appendix A. Supplementary data

Supplementary data to this article can be found online at https://doi.org/10.1016/j.jaut.2025.103372.

Data availability

links to analysis code and results are provided in the manuscript

References

[1] E. De Smit, A.J. Palmer, A.W. Hewitt, Projected worldwide disease burden from giant cell arteritis by 2050, J. Rheumatol. 42 (2015) 119–125, https://doi.org/10.3899/jrheum.140318.

[2] N.J.M. Chaddock, C.J. Harden, L. Sorensen, H.R. Mathieson, M. Zulcinski, K. Lawson, E. O'Sullivan, S. Mollan, J. Martin, S.L. Mackie, M.M. Iles, A. W. Morgan, On behalf of the UKGCA Consortium. Age, anti-coagulants, hypertension and cardiovascular genetic traits predict cranial ischaemic complications in patients with giant cell arteritis, Ann. Rheum. Dis. (2024), https://doi.org/10.1136/ard-2024-225515. Oct 3:ard-2024-225515.

[3] S.L. Mackie, E.M.A. Hensor, A.W. Morgan, C.T. Pease, Should I send my patient with previous giant cell arteritis for imaging of the thoracic aorta? A systematic literature review and meta-analysis, Ann. Rheum. Dis. 73 (2014) 143–148, https://doi.org/10.1136/annrheumdis-2012-202145.

[4] J.H. Stone, K. Tuckwell, S. Dimonaco, et al., Trial of tocilizumab in giant-cell arteritis, N. Engl. J. Med. 377 (2017) 317–328, https://doi.org/10.1056/NEJMoa1613849.

[5] S. Unizony, L. Arias-Urdaneta, E. Miloslavsky, et al., Tocilizumab for the treatment of large-vessel vasculitis (giant cell arteritis, Takayasu arteritis) and polymyalgia rheumatica, Arthritis Care Res. 64 (2012) 1720–1729, https://doi.org/10.1002/acr.21750.

[6] F. Ciccia, F. Macaluso, D. Mauro, G.F. Nicoletti, S. Croci, C. Salvarani, New insights into the pathogenesis of giant cell arteritis: are they relevant for precision medicine? Lancet Rheumatol 3 (2021) e874–e885, https://doi.org/10.1016/S2665-9913(21)00253-8.

[7] C.M. Weyand, J.J. Goronzy, Immunology of giant cell arteritis, Circ. Res. 132 (2023) 238–250, https://doi.org/10.1161/CIRCRESAHA.122.322128.

[8] H. Greigert, C. Genet, A. Ramon, B. Bonnotte, M. Samson, New insights into the pathogenesis of giant cell arteritis: mechanisms involved in maintaining vascular inflammation, J. Clin. Med. 11 (2022) 2905, https://doi.org/10.3390/jcm11102905.

[9] F.D. Carmona, S.L. Mackie, J.E. Martín, et al., A large-scale genetic analysis reveals a strong contribution of the HLA class II region to giant cell arteritis susceptibility, Am. J. Hum. Genet. 96 (2015) 565–580, https://doi.org/10.1016/j.ajhg.2015.02.009.

[10] F.D. Carmona, A. Vaglio, S.L. Mackie, et al., A genome-wide association study identifies risk alleles in plasminogen and P4HA2 associated with giant cell arteritis, Am. J. Hum. Genet. 100 (2017) 64–74, https://doi.org/10.1016/j.ajhg.2016.11.013.

[11] F.D. Carmona, P. Coit, G. Saruhan-Direskeneli, et al., Analysis of the common genetic component of large-vessel vasculitides through a meta-Immunochip strategy, Sci. Rep. 7 (2017) 43953, https://doi.org/10.1038/srep43953.

[12] R.H. Cadena, W.H. Abdulahad, G.A.P. Hospers, et al., Checks and balances in autoimmune vasculitis, Front. Immunol. 9 (2018) 315, https://doi.org/10.3389/fimmu.2018.00315.

[13] H. Zhang, R. Watanabe, G.J. Berry, et al., Immunoinhibitory checkpoint deficiency in medium and large vessel vasculitis, Proc. Natl. Acad. Sci. U.S.A. 114 (2017) E970–E979, https://doi.org/10.1073/pnas.1616848114.

[14] R. Watanabe, G.J. Berry, D.H. Liang, et al., Cellular signalling pathways in medium and large vessel vasculitis, Front. Immunol. 11 (2020) 587089, https://doi.org/10.3389/fimmu.2020.587089.

[15] C.M. Weyand, J. Schönberger, U. Oppitz, et al., Distinct vascular lesions in giant cell arteritis share identical T cell clonotypes, J. Exp. Med. 179 (1994) 951–960, https://doi.org/10.1084/jem.179.3.951.

[16] V. Martinez-Taboada, N.N. Hunder, G.G. Hunder, et al., Recognition of tissue residing antigen by T cells in vasculitic lesions of giant cell arteritis, J. Mol. Med. Berl. Ger. 74 (1996) 695–703, https://doi.org/10.1007/s001090050074.

[17] C. Schaufelberger, R. Andersson, E. Nordborg, et al., An uneven expression of T cell receptor V genes in the arterial wall and peripheral blood in giant cell arteritis, Inflammation 31 (2008) 372–383, https://doi.org/10.1007/s10753-008-9088-9.

[18] A. Brack, A. Geisler, V.M. Martinez-Taboada, et al., Giant cell vasculitis is a T cell-dependent disease, Mol. Med. 3 (1997) 530–543, https://doi.org/10.1007/BF03401699.

[19] C. Ponte, P.C. Grayson, J.C. Robson, et al., American college of rheumatology/EULAR classification criteria for giant cell arteritis, Arthritis Rheumatol. 74 (2022) 1881–1889, https://doi.org/10.1002/art.42325, 2022.

[20] B.L. Browning, S.R. Browning, A unified approach to genotype imputation and haplotype-phase inference for large data sets of trios and unrelated individuals, Am. J. Hum. Genet. 84 (2009) 210–223, https://doi.org/10.1016/j.ajhg.2009.01.005.

[21] J.J.M. van Dongen, A.W. Langerak, M. Brüggemann, et al., Design and standardization of PCR primers and protocols for detection of clonal immunoglobulin and T-cell receptor gene recombinations in suspect lymphoproliferations: report of the BIOMED-2 Concerted Action BMH4-CT98-3936, Leukemia 17 (2003) 2257–2317, https://doi.org/10.1038/sj.leu.2403202.

[22] H.S. Robins, P.V. Campregher, S.K. Srivastava, et al., Comprehensive assessment of T-cell receptor beta-chain diversity in alphabeta T cells, Blood 114 (2009) 4099–4107, https://doi.org/10.1182/blood-2009-04-217604.

[23] A. Samson, E.J. West, J. Carmichael, et al., Neoadjuvant intravenous oncolytic vaccinia virus therapy promotes anticancer immunity in patients, Cancer Immunol. Res. 10 (2022) 745–756, https://doi.org/10.1158/2326-6066.CIR-21-0171.

[24] D.A. Bolotin, S. Poslavsky, I. Mitrophanov, et al., MiXCR: software for comprehensive adaptive immunity profiling, Nat. Methods 12 (2015) 380–381, https://doi.org/10.1038/nmeth.3364.

[25] D.A. Bolotin, S. Poslavsky, A.N. Davydov, et al., Antigen receptor repertoire profiling from RNA-seq data, Nat. Biotechnol. 35 (2017) 908–911, https://doi.org/10.1038/nbt.3979.

[26] V. Giudicelli, P. Duroux, C. Ginestoux, et al., IMGT/LIGM-DB, the IMGT® comprehensive database of immunoglobulin and T cell receptor nucleotide sequences, Nucleic Acids Res. 34 (2006) D781–D784, https://doi.org/10.1093/nar/gkj088.

[27] R. Li, M. Altan, A. Reuben, et al., A novel statistical method for decontaminating T-cell receptor sequencing data, Briefings Bioinf. 24 (2023), https://doi.org/10.1093/bib/bbad230 bbad230.

[28] E.K. Morris, T. Caruso, F. Buscot, et al., Choosing and using diversity indices: insights for ecological applications from the German Biodiversity Exploratories, Ecol. Evol. 4 (2014) 3514–3524, https://doi.org/10.1002/ece3.1155.

[29] P. Dash, A.J. Fiore-Gartland, T. Hertz, et al., Quantifiable predictive features define epitope-specific T cell receptor repertoires, Nature 547 (2017) 89–93, https://doi.org/10.1038/nature22383.

[30] Z. Yu, H. Chen, J. Liu, et al., Hybrid k -nearest neighbor classifier, IEEE Trans. Cybern. 46 (2016) 1263–1275, https://doi.org/10.1109/TCYB.2015.2443857.

[31] K. Järvelin, J. Kekäläinen, Cumulated gain-based evaluation of IR techniques, ACM Trans. Inf. Syst. 20 (2002) 422–446, https://doi.org/10.1145/582415.582418.

[32] M. Girvan, M.E.J. Newman, Community structure in social and biological networks, Proc. Natl. Acad. Sci. USA 99 (2002) 7821–7826, https://doi.org/10.1073/pnas.122653799.

[33] M. Goncharov, D. Bagaev, D. Shcherbinin, et al., VDJdb in the pandemic era: a compendium of T cell receptors specific for SARS-CoV-2, Nat. Methods 19 (2022) 1017–1019, https://doi.org/10.1038/s41592-022-01578-0.

[34] C. Krishna, D. Chowell, M. Gönen, et al., Genetic and environmental determinants of human TCR repertoire diversity, Immun. Ageing 17 (2020) 26, https://doi.org/10.1186/s12979-020-00195-9.

[35] O.V. Britanova, E.V. Putintseva, M. Shugay, et al., Age-related decrease in TCR repertoire diversity measured with deep and normalized sequence profiling, J. Immunol. 192 (2014) 2689–2698, https://doi.org/10.4049/jimmunol.1302064.

[36] C. Salvarani, S.E. Gabriel, W.M. O'Fallon, G.G. Hunder, The incidence of giant cell arteritis in Olmsted County, Minnesota: apparent fluctuations in a cyclic pattern, Ann. Intern. Med. 123 (1995) 192–194, https://doi.org/10.7326/0003-4819-123-3-199508010-00006.

[37] M.A. Cimmino, R. Caporali, C.M. Montecucco, et al., A seasonal pattern in the onset of polymyalgia rheumatica, Ann. Rheum. Dis. 49 (1990) 521–523, https://doi.org/10.1136/ard.49.7.521.

[38] L. Smeeth, C. Cook, A.J. Hall, Incidence of diagnosed polymyalgia rheumatica and temporal arteritis in the United Kingdom, 1990-2001, Ann. Rheum. Dis. 65 (2006) 1093–1098, https://doi.org/10.1136/ard.2005.046912.

[39] P. Duhaut, S. Bosshard, A. Calvet, et al., Giant cell arteritis, polymyalgia rheumatica, and viral hypotheses: a multicenter, prospective case-control study.

Groupe de Recherche sur l'Artérite à Cellules Géantes, J. Rheumatol. 26 (1999) 361–369.
[40] M.A. Cimmino, G. Grazi, M. Balistreri, S. Accardo, Increased prevalence of antibodies to adenovirus and respiratory syncytial virus in polymyalgia rheumatica, Clin. Exp. Rheumatol. 11 (1993) 309–313.
[41] P. Elling, A.T. Olsson, H. Elling, Synchronous variations of the incidence of temporal arteritis and polymyalgia rheumatica in different regions of Denmark; association with epidemics of Mycoplasma pneumoniae infection, J. Rheumatol. 23 (1996) 112–119.
[42] A.D. Wagner, H.C. Gérard, T. Fresemann, et al., Detection of Chlamydia pneumoniae in giant cell vasculitis and correlation with the topographic arrangement of tissue-infiltrating dendritic cells, Arthritis Rheum. 43 (2000) 1543–1551, https://doi.org/10.1002/1529-0131(200007)43:7<1543::AID-ANR19>3.0.CO;2-8.
[43] A. Giardina, A. Rizzo, A. Ferrante, et al., Giant cell arteritis associated with chronic active Epstein-Barr virus infection, Reumatismo 65 (2013) 36–39, https://doi.org/10.4081/reumatismo.2013.36.
[44] S.E. Gabriel, M. Espy, D.D. Erdman, et al., The role of parvovirus B19 in the pathogenesis of giant cell arteritis: a preliminary evaluation, Arthritis Rheum. 42 (1999) 1255–1258, https://doi.org/10.1002/1529-0131(199906)42:6<1255::AID-ANR23>3.0.CO;2-P.
[45] M.A. Nagel, T. White, N. Khmeleva, et al., Analysis of varicella-zoster virus in temporal arteries biopsy positive and negative for giant cell arteritis, JAMA Neurol. 72 (2015) 1281–1287, https://doi.org/10.1001/jamaneurol.2015.2101.
[46] R.A. Ostrowski, S. Metgud, R. Tehrani, W.M. Jay, Varicella zoster virus in giant cell arteritis: a review of current medical literature, Neuro-Ophthalmol Aeolus Press 43 (2019) 159–170, https://doi.org/10.1080/01658107.2019.1604763.
[47] E. Nordborg, C. Nordborg, Giant cell arteritis: epidemiological clues to its pathogenesis and an update on its treatment, Rheumatology 42 (2003) 413–421, https://doi.org/10.1093/rheumatology/keg116.
[48] C.A. Langford, D. Cuthbertson, S.R. Ytterberg, et al., A randomized, double-blind trial of abatacept (CTLA-4Ig) for the treatment of giant cell arteritis, Arthritis Rheumatol. 69 (2017) 837–845, https://doi.org/10.1002/art.40044.
[49] M.J. Koster, C.S. Crowson, R.E. Giblon, et al., Baricitinib for relapsing giant cell arteritis: a prospective open-label 52-week pilot study, Ann. Rheum. Dis. 81 (2022) 861–867, https://doi.org/10.1136/annrheumdis-2021-221961.